Single-End Crosstalk Measurement Method for Multi-Core Fibers Using Continuous Light Source

Yuto Yamaguchi, Ayumi Inoue, Takahiro Kikuchi, Takuji Nagashima, Hidehisa Tazawa, Tetsuya Hayashi
Optical Communications Laboratory, Sumitomo Electric Industries, Ltd., 1, Taya-cho, Sakae-ku, Yokohama 244-8588, Japan
yamaguchi-yuto@sei.co.jp, t-hayashi@sei.co.jp

Abstract: We propose multi-core fiber (MCF) crosstalk measurement method which requires only one fan-in/fan-out at a single end of MCF, and is applicable to short MCFs whose crosstalk is difficult to be measured using OTDR method.

1. Introduction

Space division multiplexing (SDM) is a promising technology to increase the transmission capacity of optical networks [1], and the multicore fiber (MCF) has been finally commercialized for submarine applications [2]. Also for terrestrial applications, MCF technology has progressed for practical applications, and the MCFs with standard 125-µm cladding or 250-µm coating [3–5] and MCF high-density cables [5–7] have been demonstrated. To commercialize such high-density terrestrial MCF cables, efficient inter-core crosstalk (XT) measurement is necessary. Transmission method [8,9] is the most basic and widely used measurement method for the XT of MCFs, but we have to access the both ends of the cores. Therefore, to evaluate the XT of a high MCF count cable, the both ends of each single MCF have to be simultaneously identified from hundreds/thousands of MCFs and aligned to fan-in/fan-outs (FIFOs) at the same time. The optical time domain reflectometry (OTDR) method [10,11] is another XT measurement method that can measure the XT with single-end FIFO connection, which could simplify the MCF handling and FIFO connection during MCF cable testing. However, the OTDR method requires kilometer-order pulse length (10 to 20 µs in time domain) to evaluate extremely weak backscattered power of the XT, and may not be suitable for XT evaluation of short MCFs in high-density cables whose lengths are often a few kilometers or shorter. An OTDR measurement with loopback configuration [12] can use shorter pulses, but this method requires FIFO connection/splicing at both ends of an MCF, thus does not simplify the MCF handling and FIFO connection.

In this paper, we propose a single-end XT measurement method, which uses a continuous light source and evaluates the powers of the backward propagating lights in an MCF, and can be applied to short MCFs whose XT is difficult to be measured using the OTDR method.

2. Principle

We express the XT using the symbols shown in Fig. 1a. In line with literature, the XT of forward propagating power from Core 1 to Core 2 can be expressed as $\mathrm{XT}_{\mathrm{f},21} = F_{21}/F_{11}$, where F_{mn} is the element of the power transfer matrix of forward propagating light in the cores. By taking the geometric mean of the linear values (or the arithmetic mean of the decibel values), we can remove the effect of the core dependent loss (CDL) on the XT, and the XT between Core 1 and Core 2 can be expressed as [9]: $\mathrm{XT}_\mathrm{f} \equiv \sqrt{\mathrm{XT}_{\mathrm{f},21}\mathrm{XT}_{\mathrm{f},12}} = hL$, where h is the power coupling coefficient between Core 1 and Core 2, and L is the fiber length. In this study, we define *backward XT* as

$$\mathrm{XT}_\mathrm{b} \equiv \sqrt{\mathrm{XT}_{\mathrm{b},21}\mathrm{XT}_{\mathrm{b},12}}, \quad \mathrm{XT}_{\mathrm{b},21} = B_{21}/B_{11} \tag{1}$$

based on the backward-direction output powers in an MCF (See Fig. 1a). Note that the backward XT is defined just for measurement purpose, and different from the counter-propagating XT [4]. The backward propagating powers can be induced by the Fresnel reflection at the non-input end of the MCF as fiber under test (FUT) (Fig. 1b), and by Rayleigh backscattering along the MCF (Fig. 1c). XT_b can be expressed as ($B_{\mathrm{bs},mn}$ can be derived from Eq. (12) in [13] by integration along the MCF with some approximation and algebraic manipulation. Core-dependent optical properties of the MCF are ignored for discussion simplicity):

$$\mathrm{XT}_\mathrm{b} \simeq \mathrm{XT}_{\mathrm{b},21} = \frac{B_{21}}{B_{11}} = \frac{B_{\mathrm{refl},21} + B_{\mathrm{bs},21}}{B_{\mathrm{refl},11} + B_{\mathrm{bs},11}} \approx \frac{2hLR_\mathrm{end}\exp(-2\alpha L) + hL\frac{S\alpha_\mathrm{R}}{\alpha}\left[\frac{1-\exp(-2\alpha L)}{2\alpha L} - \exp(-2\alpha L)\right]}{R_\mathrm{end}\exp(-2\alpha L) + \frac{S\alpha_\mathrm{R}}{\alpha}\left[\frac{1-\exp(-2\alpha L)}{2}\right]} = \mathrm{XT}_\mathrm{f}\frac{2R_\mathrm{end} + \frac{S\alpha_\mathrm{R}}{\alpha}\left[\frac{\exp(2\alpha L)-1}{2\alpha L} - 1\right]}{R_\mathrm{end} + \frac{S\alpha_\mathrm{R}}{\alpha}\left[\frac{\exp(2\alpha L)-1}{2}\right]} \tag{2}$$

where R_end is the reflectivity of the non-input end facet of the FUT, α is the propagation loss coefficient of optical power, α_R is the Rayleigh scattering loss coefficient, and S is the proportion of the Rayleigh scattering component recaptured into a backward direction. Under the Gaussian field approximation [14], polarization-averaged R_end of the Fresnel reflection with the cleave angle θ [rad] can be approximated as

$$R_\mathrm{end} \approx \left[\left(n_\mathrm{fiber} - n_\mathrm{air}\right)/\left(n_\mathrm{fiber} + n_\mathrm{air}\right)\right]^2 \exp\left[-\left(2\pi n_\mathrm{fiber} w\theta/\lambda\right)^2\right] \tag{3}$$

where n_fiber and n_air are the refractive indices of the FUT and air, w is the spot size, and λ is the wavelength in vacuum. The loss coefficients α and α_R can be converted to decibel parameters by multiplying 10/ln10 ~ 4.34. The Rayleigh re-capturing factor can be expressed $S \simeq 3\pi/(2k^2n^2A_{\mathrm{eff}}) \simeq 3/(2k^2n^2w^2)$ [13,14], where $k = 2\pi/\lambda$, n is the refractive index, A_{eff} is the nonlinear effective area. From Eq. (2), the ratio of the backward XT to the forward XT depends on R_{end} and αL. By using the $\mathrm{XT_b/XT_f}$ value calculated using Eq. (2), $\mathrm{XT_f}$ can be evaluated from measured $\mathrm{XT_b}$ value. Figure 1d shows the example of the dependence of $\mathrm{XT_b/XT_f}$ on R_{end} and αL, at $\lambda = 1.55$ µm of an MCF whose core design is compatible to ITU-T G.657.A1 where we assumed α is 0.19 dB/km, α_R is 0.17 dB/km, $w = 5$ µm, $A_{\mathrm{eff}} = 75$ µm^2, $n_{\mathrm{fiber}} = 1.45$, and $n_{\mathrm{air}} = 1$. When αL is low, $\mathrm{XT_b/XT_f}$ is approximately 2 (~3 dB) in reflection dominant case and 1 (0 dB) in backscattering dominant case. As αL increases, $\mathrm{XT_b/XT_f}$ gradually decreases in backscattering dominant case. Even if R_{end} is not very low—like −14.7 dB (Fresnel reflection with $\theta = 0$) or 0 dB (100% reflection)—, the reflected power is attenuated with the αL increase and $\mathrm{XT_b/XT_f}$ converges to the backscattering dominant case when αL in dB is > 20 to 30. In reflection/backscattering dominant cases, Eq. (2) can be approximated to

$$\mathrm{XT_b} \approx \begin{cases} B_{\mathrm{refl},21}/B_{\mathrm{refl},11} = 2\mathrm{XT_f}, & \text{(Reflection dominant case)} \\ B_{\mathrm{bs},21}/B_{\mathrm{bs},11} = \mathrm{XT_f}\left\{1/\alpha L - 2/\left[\exp(2\alpha L)-1\right]\right\}, & \text{(Backscattering dominant case)} \end{cases} \quad (4)$$

where R_{end} and $S\alpha_R/\alpha$ are cancelled out in both cases.

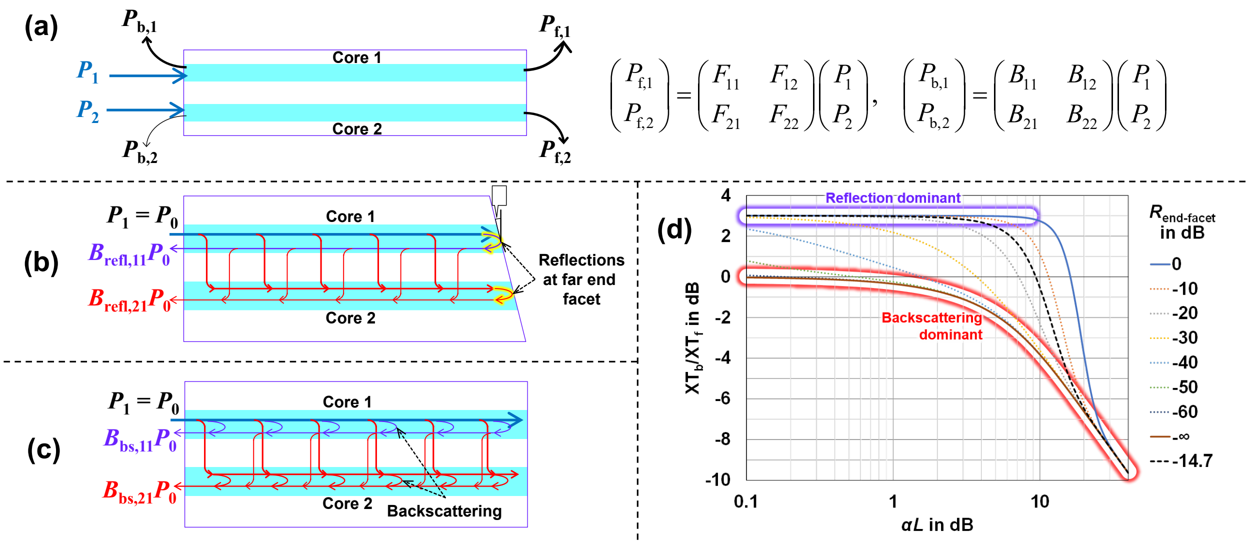

Figure 1. Schematic illustrations depicting (a) forward and backward propagating power transfers for XT definitions, (b) backward propagating power reflected at the non-input end MCF facet with cleave angle θ, and (c) backward propagating power backscattered by Rayleigh scattering. (d) The ratio of the backward XT to the forward XT vs. the transmission loss αL and the reflectivity R_{end}, at $\lambda = 1.55$ µm of an MCF with core design compatible to ITU-T G.657.A1.

3. Measurement and discussion

Figure 2a shows the setup for the proposed single-end XT measurement method. The continuous light is launched into a core of the MCF (FUT) via input/output (I/O) section (an optical switch, an optical circulator, and a FIFO device). The light propagates in the FUT, couples to other cores, backscattered and reflected. Then, the backward propagating lights are received by an optical power meter via the I/O components (the FIFO, optical circulators, and another optical switch). Although the I/O section (including the fusion splice between the FIFO pigtail and the FUT) have CDL and the measured value of $\mathrm{XT_b}$ can be affected by the CDL as:

$$\mathrm{XT}_{\mathrm{b},21}^{\mathrm{meas}} = \left(B_{21}^{\mathrm{meas}}P_0\right)\Big/\left(B_{11}^{\mathrm{meas}}P_0\right) \approx \left(F_{22}^{\mathrm{out}}B_{21}^{\mathrm{FUT}}F_{11}^{\mathrm{in}}P_0\right)\Big/\left(F_{11}^{\mathrm{out}}B_{11}^{\mathrm{FUT}}F_{11}^{\mathrm{in}}P_0\right), \quad (5)$$

the CDL effects can be cancelled by the geometric mean of the linear values (or the arithmetic mean of the decibel values) as $\sqrt{\mathrm{XT}_{\mathrm{b},21}^{\mathrm{meas}}\mathrm{XT}_{\mathrm{b},12}^{\mathrm{meas}}} \approx \sqrt{\mathrm{XT}_{\mathrm{b},21}^{\mathrm{FUT}}\mathrm{XT}_{\mathrm{b},12}^{\mathrm{FUT}}}$. F_{nn}^{out} and F_{nn}^{in} are F of the I/O section in the output and input directions.

The FUT was the step-index 4-core fiber with core design compatible to ITU-T G.657.A1 with 3 different length, whose properties are summarized in Table 1. We used etched taper bundle type FIFOs [15] using trench-assisted 4-core fibers, which can realize negligibly low return loss and negligibly low forward and return XT (Fig. 2b). The MCF pigtail of the FIFO and the MCF (FUT) were fusion spliced for suppressing the return loss at the connection. The optical switches also have negligibly low XT. Therefore, the possible source of the measurement error is the XT in the optical circulator from port 1 to port 3 (Fig. 2c). In the measurement setup, the ratio $X_{nn}^{\mathrm{I/O}}$ of the XT from input to output in the same channel n of the I/O section without the FUT was less than −50 dB (including the effect of switch insertion loss). In backscattering dominant case with a short FUT, $X_{11}^{\mathrm{I/O}}P_0$ is not negligible compared to the backward

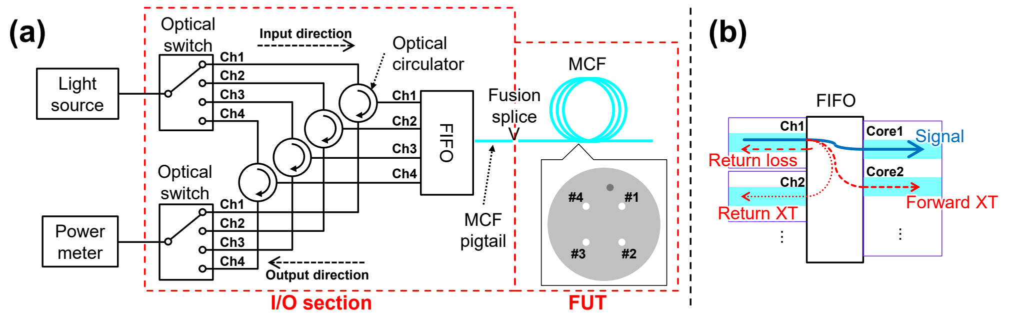

Figure 2. (a) Setup for the single-end XT measurement. (b,c) Noise sources for the measurement in (b) FIFO and (c) circulator.

Table 1. Properties of the 4-core fiber samples used for the single-end XT measurement method validation.

	Length [km]	λ_{cc} [a] [nm]	MFD[a,b] [μm]	MFD1[a,b] [μm]	A_{eff} [a,b] [μm^2]	α [a,b] in dB/km	α_R [a,b] in dB/km	XT_f/L [a,b] in dB at 1 km	Core pitch [μm]	Clad diam. [μm]
FUT-1	1.23	1264	9.5	9.8	71	0.19	0.17	−43.3	40	125
FUT-2	7.77	1249	9.8	10.0	75	0.19	0.17	−35.5		
FUT-3	43.47	1258	9.8	10.0	75	0.19	0.17	−37.0		

a) average of 4 cores, b) at λ = 1.55 μm.

propagating power from the through core of the FUT ($F_{11}^{\mathrm{out}}B_{11}^{\mathrm{FUT}}F_{11}^{\mathrm{in}}P_0$, the denominator in Eq. (5)). Therefore, the effect of $X_{11}^{\mathrm{I/O}}P_0$ was subtracted from $B_{11}^{\mathrm{meas}}P_0 \approx F_{11}^{\mathrm{out}}B_{11}^{\mathrm{FUT}}F_{11}^{\mathrm{in}}P_0 + X_{11}^{\mathrm{I/O}}P_0$ to obtain $F_{11}^{\mathrm{out}}B_{11}^{\mathrm{FUT}}F_{11}^{\mathrm{in}}P_0$.

We investigated the accuracy of the proposed measurement method in a reflection-assisted (R-assisted) case ($\theta \sim 0$ [deg]) and a reflection-suppressed (R-suppressed) case ($\theta \sim 8$ [deg], $R_{\mathrm{end}} << -60$ dB). The non-input end of the FUT was cleaved using a commercial high-precision fiber cleaver to control θ. Table 2 summarizes the XT measurement results, which clearly shows the accuracy of the single-end measurement method in the R-assisted case. In the R-suppressed case, XT_f measured using the single-end method were slightly lower than the reference XT_f by the transmission method, and the measurement error becomes larger with lower αL, or shorter FUT. However, the maximum value of |(average) ± 3×(standard deviation)| of the measurement errors were still <2 dB. Further studies are necessary to reveal the cause of the measurement error in the R-suppressed case, but the lower backward propagating powers may make the measurement sensitive to various noises.

Table 2. Measurement results of the XT using the transmission method and the single-end measurement method.

	αL in dB[a]	Transmission method (reference) (i) **XT_f in dB**[a] (measured)	Proposed single-end method (ii) XT_b in dB [a] (measured)		(iii) XT_b/XT_f in dB (calculated using (2,3))		(iv) **XT_f in dB**[a] [(ii)−(iii)]		**Measurement error [dB]**[b] [(iv) − (i)]	
			R-assisted	R-suppressed	R-assisted	R-suppressed	**R-assisted**	**R-suppressed**	**R-assisted**	**R-suppressed**
FUT-1	0.23	**−42.42**	−39.47	−43.36[c]	3.00	−0.08	**−42.48**	**−43.28**[c]	**−0.06 ± 0.07**	**−0.86 ± 0.29**[c]
FUT-2	1.47	**−26.56**	−23.65	−27.50	2.95	−0.52	**−26.61**	**−26.99**	**−0.05 ± 0.04**	**−0.43 ± 0.10**
FUT-3	8.22	**−20.59**	−19.74	−24.06	0.86	−3.17	**−20.60**	**−20.89**	**−0.01 ± 0.03**	**−0.30 ± 0.08**

*at λ = 1.55 μm, a) average value of 4 pairs of nearest-neighboring cores, b) average ± standard deviation of the measurement errors of 4 pairs of nearest-neighboring cores, c) the powers of circulator XT were subtracted to reduce the measurement error.

4. Conclusion

We proposed a single-end XT measurement method using continuous light source and capable of evaluating MCFs whose length is a few kilometers or shorter. The proposed method was experimentally validated with the 4-core fibers with core design compatible to ITU-T G.657.A1 for the fiber length from 1.23 km to 43.47 km. Especially, assisted with Fresnel reflection at non-input end of the FUT, the proposed method demonstrated excellent accuracy. Although the minimum fiber length in the experiment was 1.23 km, the proposed method may be also applicable to the XT measurement of further shorter MCFs and various multicore devices such like FIFO if we can utilize the Fresnel reflection at the non-input end. The proposed method will realize single-end accurate XT measurement of multicore fibers/devices whilst overcoming the minimum fiber length limit of the OTDR method, and will enable efficient XT evaluation of high-fiber-count MCF cables.

[1] W. Klaus *et al.*, Proc. IEEE **110**(11), 1619–1654 (2022).
[2] Sumitomo Electric Industries, Ltd., "Sumitomo Electric Launches World's First Mass-produced Ultra-low Loss, Multi-core Fiber," News release (Sep. 2023), https://sumitomoelectric.com/press/2023/09/prs049.
[3] T. Matsui *et al.*, in OFC 2021, p. Tu6B.4.
[4] T. Hayashi *et al.*, in OFC 2022, p. M1E.1.
[5] T. Hayashi *et al.*, in OFC 2023, p. Tu2C.2.
[6] T. Hayashi *et al.*, in OFC 2015, p. Th5C.6.
[7] T. Hayashi *et al.*, in IWCS 2023, pp. 193–197.
[8] T. Hayashi *et al.*, J. Lightw. Technol. **30**(4), 583–589 (2012).
[9] Y. Kobayashi *et al.*, Opt. Express **31**(1), 502–508 (2023).
[10] M. Nakazawa *et al.*, Opt. Express **20**(11), 12530–12540 (2012).
[11] Y. Kobayashi *et al.*, in ACP 2022, pp. 293–295.
[12] M. Nakagawa *et al.*, in ECOC 2022, p. Tu4A.4.
[13] T. Hayashi, Opt. Express **30**(13), 23943–23952 (2022).
[14] E. Brinkmeyer, Electronics Letters **16**(9), 329–330 (1980).
[15] T. Kikuchi *et al.*, in OECC/PSC 2022, p. TuC4-2.